Journal Pre-proof

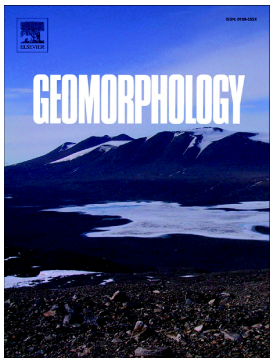

Salt marsh resilience to sea-level rise and increased storm intensity

Natascia Pannozzo, Nicoletta Leonardi, Iacopo Carnacina, Rachel Smedley

PII: S0169-555X(21)00233-6

DOI: https://doi.org/10.1016/j.geomorph.2021.107825

Reference: GEOMOR 107825

To appear in: *Geomorphology*

Received date: 7 October 2020

Revised date: 28 May 2021

Accepted date: 31 May 2021

Please cite this article as: N. Pannozzo, N. Leonardi, I. Carnacina, et al., Salt marsh resilience to sea-level rise and increased storm intensity, *Geomorphology* (2021), https://doi.org/10.1016/j.geomorph.2021.107825

Salt marsh resilience to sea-level rise and increased storm intensity

Natascia Pannozzo[a*], Nicoletta Leonardi[a], Iacopo Carnacina[b], Rachel Smedley[a]

[a]Department of Geography and Planning, School of Environmental Sciences, University of Liverpool, Chatham Street, Liverpool, L69 7ZT, UK

[b]Department of Civil Engineering, School of Civil Engineering and Built Environment, Liverpool John Moores University, Byrom Street, Liverpool, L3 3AF, UK

[*]sgnpanno@liverpool.ac.uk (corresponding author)

Abstract

Salt marshes are important ecosystems but their resilience to sea-level rise and possible increases in storm intensity is largely uncertain. The current paradigm is that a positive sediment budget supports the survival and accretion of salt marshes while sediment deprivation causes marsh degradation. However, few studies have investigated the combined impact of sea-level rise and increased storm intensity on the sediment budget of a salt marsh. This study investigates marsh resilience under the combined impact of various storm surge (0 m, 0.25 m, 0.5 m, 1.0 m, 2.0 m, 3.0 m and 4.0 m) and sea-level (+0 m, +0.3 m, +0.5 m, +0.8 m and +1.0 m) scenarios by using a sediment budget approach and the hydrodynamic model Delft3D. The Ribble Estuary, North-West England, whose salt marshes have been anthropogenically restored and have a high economic and environmental value, has been chosen as test case. We conclude that storm surges can positively contribute to the resilience of the salt marsh and estuarine system by promoting flood dominance and by triggering a net import of sediment. Conversely, sea-level rise can threaten the stability of the marsh by promoting ebb dominance and triggering a net export of sediment. Our results suggest that storm surges have a general tendency to counteract the decrease in sediment budget caused by sea-level rise. The timing of the storm surge relative to high or low tide, the duration of the surge, the change in tidal range and vegetation presence can also cause minor changes in the sediment budget.

Keywords: salt marshes, storm surges, sea-level rise, Delft3D

1. Introduction

Salt marshes are vegetated wetlands, typical of mid and high latitudes, that are distributed within the upper intertidal zone of low-energy shorelines, such as estuaries, deltas, and barrier islands (Townend et al., 2011). Salt marshes have been widely recognised as valuable coastal defences due to their ability to buffer storm waves (e.g. Möller et al. 1999; Leonardi et al., 2018). There have been a variety of projects around the world to create new salt marshes and/or restore salt marshes that were previously reclaimed for anthropogenic activities to provide long-term and low-cost coastal protection (Temmerman et al., 2013). Salt marshes also provide other valuable ecosystem services, including nutrient removal, habitat provision and high rates of carbon sequestration at geological time scales (Zedler and Kercher, 2005; Barbier et al., 2011). The fate of salt marshes is, however, uncertain as it is still unclear how salt marshes will be affected by the combined impacts of sea-level rise and intensification of storms activity, inducing higher level storm surges (Schuerch et al., 2013; IPCC, 2018). The sensitivity of tidal flat and salt marsh complexes to changes in hydrodynamics depends on a variety of local features including tidal characteristics, sediment availability, vegetation characteristics and depositional processes (Reed, 1995).

Salt marshes are generally resilient to sea-level rise when sediment supply and organogenic production are high enough to allow marsh accretion or when salt marshes can migrate upland (Kirwan et al., 2010, 2016). The accretion and encroachment of new salt marshes occurs when the delivery of fine sediments from rivers and the sea increases the elevation of marsh platforms and tidal flats relative to the sea-level, and vegetation colonises newly exposed surfaces (Reed, 1990). Sediments that arrive from the sea are delivered during flood tide and sediment deposition is determined by the duration and frequency of tidal inundation (hydroperiod) with more deposition occurring when inundation is longer and more frequent (Reed, 1990). Vegetation supports marsh stability through biomass growth, particle capture by plant stems, and enhanced particle settling

caused by a reduction in turbulent kinetic energy of the water flow through the plant canopy (Morris et al. 2002; Neumeier and Ciavola, 2004; Mudd et al., 2010). Increasing rates of sea-level rise can lead to marsh drowning by increasing the accommodation space and the amount of sediment inputs required for marsh stability (FitzGerald et al., 2008; Kirwan et al., 2010; Ganju et al., 2017). Lateral erosion by wind waves can also cause marsh degradation (Marani et al., 2011; Fagherazzi et al., 2013; Leonardi and Fagherazzi, 2014; Leonardi et al., 2018; Li et al., 2019). While waves generated during storms can contribute to salt marsh erosion, there is evidence that overwash by storm surges delivers significant amount of sediments to marsh platforms supporting marsh resilience to sea-level rise (Turner et al., 2006; Walters and Kirwan, 2016; Castagno et al., 2018). Overall, the net sediment budget of a coastal system is a useful metric to evaluate the life-span of salt marshes; a positive sediment budget is frequently associated with the capability of salt marshes to expand, while a negative sediment budget has been linked to marsh degradation (Ganju et al., 2015).

This study investigates the resilience of salt marshes to sea-level rise and storm intensification by focussing on the combined influence of increasing sea-level and storm surge height on the sediment budget of a salt marsh-tidal flat complex using a numerical model of the Ribble Estuary, North-West England. Saltmarshes in the Ribble Estuary are one of Europe's largest systems, which has been restored through managed realignment to provide flood protection (Tovey et al., 2009). A total of 250 numerical simulations representing different storm surge heights and sea-level rise magnitudes were conducted; the timing of occurrence of the surge with respect to high or low tide, the duration of the surge, the change in tidal range and vegetation presence were also considered to understand the influence of these factors on the nature and amplitude of changes in sediment budget.

2. Study site

The Ribble Estuary is located on the Lancashire coast, North-West England (Figure 1c). The estuary is funnel shaped, tidally dominated and macrotidal; the ordinary tidal range is 8.0 m at

spring tide and 4.4 m at neap tide (UKHO, 2001). The average marsh platform elevation is approximately 3.5 m above mean sea level. The estuary experiences moderate wave energy owed to waves being generated in the Irish Sea basin (Pye and Neal, 1994). It is thought that the formation of the extensive intertidal sand-silt flats and the salt marsh at the south of the estuary resulted from the combination of infilling of sandy sediments from the bed of the Irish Sea, deposition of the silt and clay-size sediments coming from the River Ribble and a moderate wave climate insufficient to cause significant lateral erosion (Van der Wal et al., 2002). Van der Wal et al. (2002) suggested that the river does not significantly influence the sediment supply to the estuary and that the sedimentation is mainly affected by marine sediment. Lyons (1997) suggested that tidal pumping, especially during high storm surges is the main process introducing sediments into the estuary. Between 2007 and 2017, a scheme was implemented to restore the intertidal habitat previously reclaimed for agricultural purposes and the area has high ecological and economic value (Tovey et al., 2009).

3. Methods

3.1 The model

The FLOW module of the numerical finite-difference model Delft3D was used to simulate the hydrodynamics and sediment transport of the system. The model calculates non-steady flow and transport phenomena using Navier-Stokes and transport equations (DELFT Hydraulics, 2014). The model accounts for bed-load and suspended-load of multiple cohesive and non-cohesive sediment fractions, vertical diffusion of sediments due to turbulent mixing and the sediment settling due to gravity. It also accounts for the effect of vegetation on the flow field. The suspended load is evaluated through the advection–diffusion equation and the bed-load transport is computed using the formulation proposed by Van Rijn (1993). The exchange of sediments between the bed and the flow for non-cohesive sediments is computed by evaluating sources and sinks of sediments near the bottom, respectively due to upward diffusion and sediments dropping out from the flow due to their

settling velocities (Van Rijn, 1993). For cohesive sediments, the Partheniades–Krone formulations for erosion and deposition are used (Partheniades, 1965). The vegetation presence is computed following the formulation of Baptists (2007). The module accounts for the three-dimensional effect of rigid cylindrical plant structures on drag and turbulence. The first is modelled by adding an extra source term of friction force, caused by the cylindrical plant structures, in the momentum equation; the second is achieved by adding an extra source term of turbulent kinetic energy dissipation, generated by the cylindrical plant structures, in the k-e equations. For more information on the vegetation module, we refer to DELFT Hydraulics (2014). The design of the domain and the set-up and calibration of the model for this study were performed by Li et al. (2018, 2019). The domain consists of a grid of 344 x 80 cells in the east to west and north to south direction (Figure 1a), and three equally spaced vertical layers. The bathymetry (Figure 1b) was obtained from the combination of two datasets: the bathymetric data for the open sea collected from EDINA DIGIMAP and the LiDAR data for the coastal regions downloaded from the Environment Agency's LiDAR data archive. Since the two datasets have different vertical reference levels, Low Astronomical Tide (LAT) and Above Ordnance Datum Newlyn (AODN) respectively, they were adjusted and referred to Mean Sea Level (MSL) following the spatially varying Vertical Offshore Reference Frame (VORF) corrections provided by the UK Hydrographic Office prior to combination. The model is constrained within two open boundaries, one 20 km offshore and one across the River Ribble. Data for the offshore boundary was provided by the Extended Area Continental Shelf Model fine grid (CS3X), which has approximately 12 km resolution, covers an area from 53.55° N to 53.92° N and from -3.33° E to -2.75° E, and uses meteorological data from the UK Met Office Operational model, consisting of hourly water level and current simulation values. Data for the river boundary was collected from the National River Flow Archive and consists of a time series of daily-averaged river discharge values; a constant discharge of 44 m^3/s was estimated using the mean discharge for the simulated period. Measurements of suspended sediment concentration performed in the Ribble Estuary by Wakefield et al. (2011) were used to estimate a constant sediment discharge from the

river of 0.29 kg/m^{3}s. A restricted area of the domain was selected for the sediment budget calculation (Figure 1). For more information on model setup and calibration we refer to Li et al. (2018, 2019).

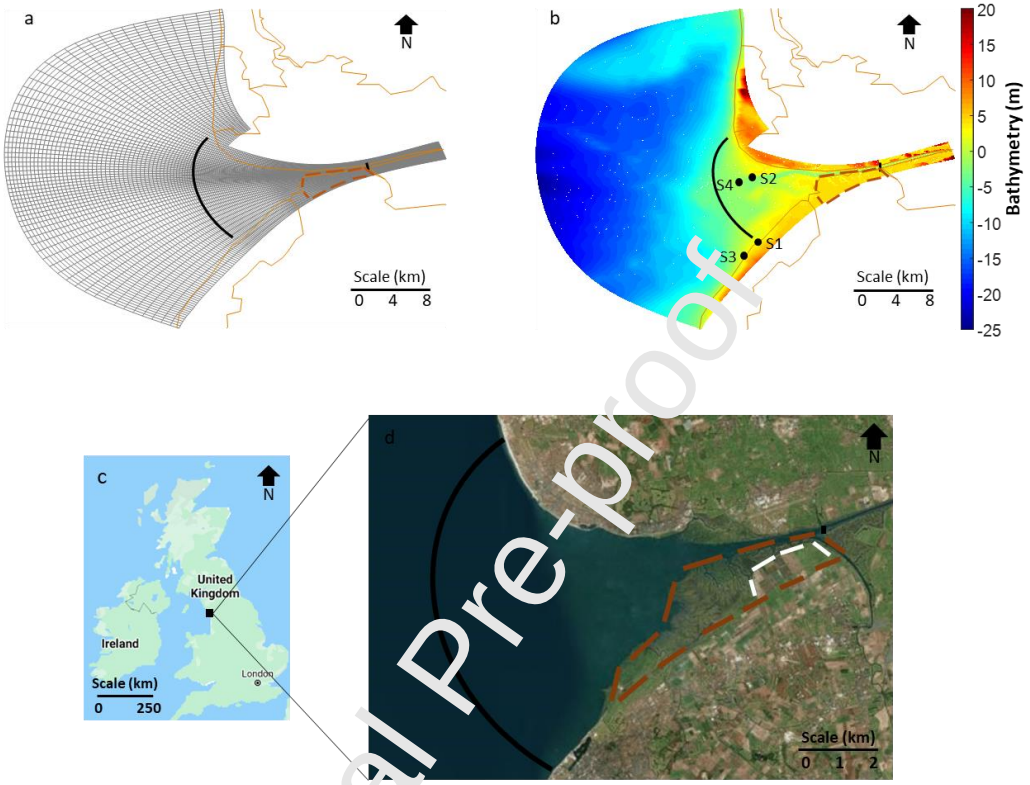

Figure 1. Grid (a), bathymetry (b) and map (c, d) of the domain. The continuous brown lines represent the land boundary. The area enclosed by the black curved lines and the area enclosed by the brown dashed lines (panel a, b and d) are respectively the restricted domain and the salt marsh used for the calculation of the cumulative sediment deposition. The area enclosed by the white dashed lines (panel d) is now part of the saltmarsh as it was restored in 2017 (RSPB, 2019). In panel b, the yellow shade corresponds to the tidal flat and nearshore area, the green shade corresponds to the inner estuary and the light blue shade corresponds to the outer estuary.

3.2 Simulation scenarios and tidal analysis

A total of 250 simulations were conducted (Table 1). Each simulation was run for a month from January 1st until January 31st 2008. The maximum spring and neap high tides in this period reach respectively 4.2 m and 3.2 m above mean sea-level and the minimum spring and neap low tides

reach respectively 3.8 m and 2.5 m below mean sea-level. Storm surges that characterise mid-high latitudes have a typical duration of 2-5 days (von Storch et al., 2015). To understand the impact of the storm duration on the sediment budget, gaussian functions with duration 48 hours (σ = 6 hours), 72 hours (σ = 9 hours) and 120 hours (σ = 15 hours) were added to the initial water level time series at the offshore boundary. Extreme value analysis of storm surge residuals along the UK coastline, presented in Table 1 by Pannozzo et al. (2021), showed surge heights up to 3 m for exceedance probabilities p=0.01. Values at regular intervals within the range of these observations were chosen to simulate storm surges of different heights: 0 m, 0.25 m, 0.5 m, 1.0 m, 2.0 m, 3.0 m and 4.0 m (Figure 2a and 2b). To understand the role of the timing of the surge with respect to tidal levels, for each surge height, two runs were conducted, one with the peak of the surge coinciding with the peak of high tide and one with the peak of the surge coinciding with the peak of low tide. To understand the role of tidal range, these scenarios were simulated for both spring and neap tide. The storm surge was introduced after 11 days of simulation for the spring tide scenario and after 18 days for the neap tide scenario, to avoid any interference with the initial spin-up time. To simulate different sea-level scenarios, the bathymetry was lowered by 0 m, 0.3 m, 0.5 m, 0.8 m and 1.0 m (Figure 2c). These values were chosen as regular intervals within the range of the IPCC scenarios (IPCC, 2018). The whole bathymetry was modified, without accounting for morphodynamic evolution. This has been done in previously published papers to simulate scenarios of higher sea-level (e.g. Zhang et al., 2020). Storm surges and sea-level scenarios were then combined to investigate the integrated effects on the sediment budget; the 48 hours scenarios occurring during spring tide were used for this purpose. The Ribble Estuary experiences moderate wave energy (Pye and Neal, 1994). However, for simplicity, the effects of wind waves have been neglected in this study to investigate exclusively the distinct effects of surges and sea-level. There is evidence that vegetation affects sediment deposition not only directly, by capturing particles and enhancing particle settling, but also indirectly, by changing the water flow direction and increasing the flood velocity, hence causing sediment resuspension (Temmermann et al., 2005). Simulations were

conducted with and without vegetation presence to test how it affects sediment deposition and, ultimately, the sediment budget. A plant density of 512 stems/m^2 was used for the vegetated scenarios to simulate a high level of vegetation cover (Li et al., 2018). The cumulative sediment deposition across the marsh area and estuarine system within the restricted domain was used as an estimate of the sediment budget and describes the amount of accretion (positive values) or erosion (negative values) of the bed for each cell of the domain. The net accretion/erosion on the whole marsh and restricted domain can be calculated by multiplying the cumulative deposition of each cell for the cell area and summing them, making it a useful proxy to determine the amount of sediment stored within the system.

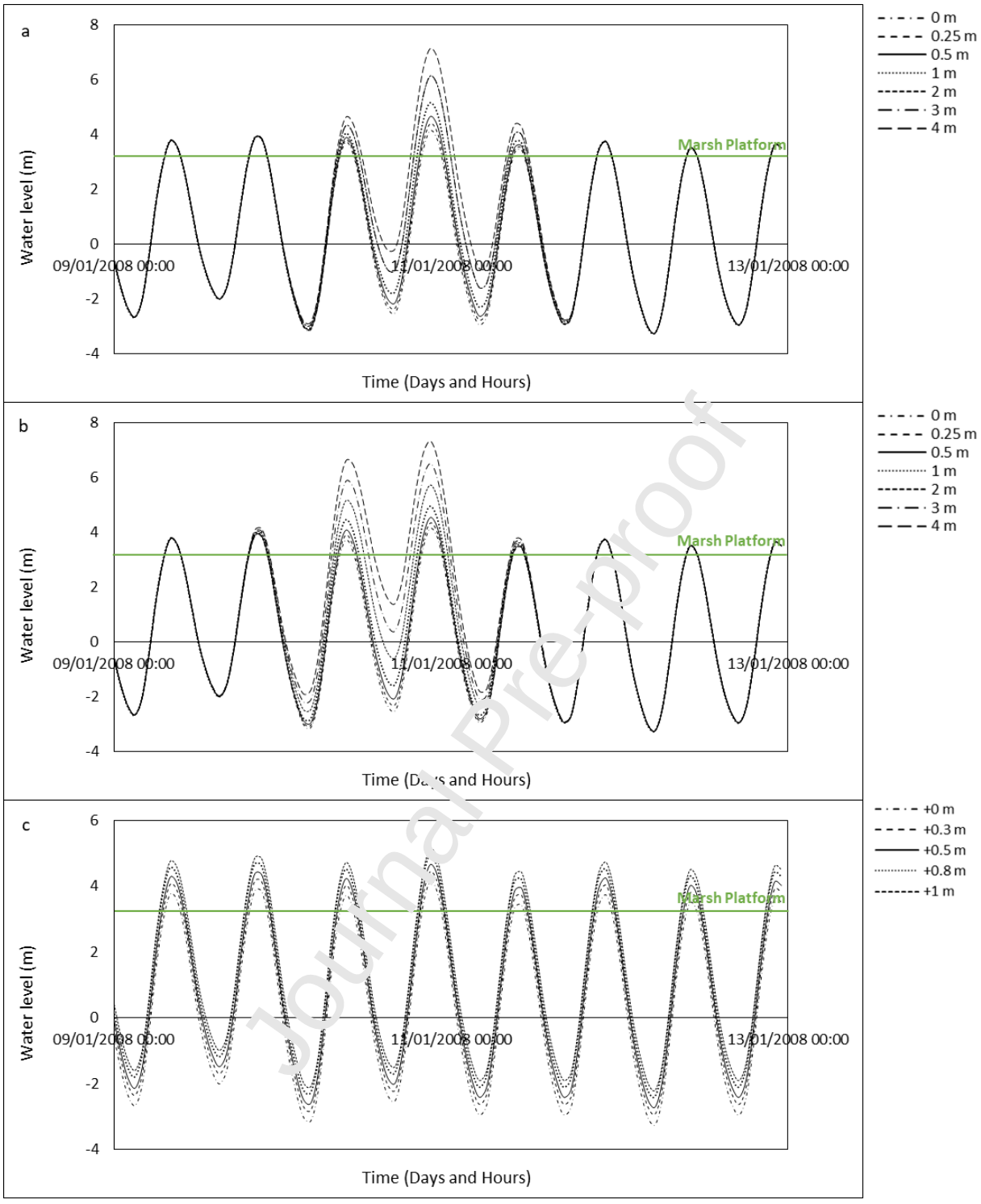

Figure 2. Water level for scenarios of surges peaking at high (a) and low (b) tide; the 48 hours scenarios occurring during spring tide is used for the illustration. Water level for scenarios of different sea-levels (c); five days during spring tide were selected for the illustration. The water level is calculated as an average of all water levels at the ocean open boundary.

Sea-level scenarios	Storm surges scenarios at HT and LT peak (for durations of 48hr, 72 hr, 120 hr)						
0 m	0 m	0.25 m	0.5 m	1 m	2 m	3 m	4 m
0.3 m	0 m	0.25 m	0.5 m	1 m	2 m	3 m	4 m
0.5 m	0 m	0.25 m	0.5 m	1 m	2 m	3 m	4 m
0.8 m	0 m	0.25 m	0.5 m	1 m	2 m	3 m	4 m
1 m	0 m	0.25 m	0.5 m	1 m	2 m	3 m	4 m

Table 1. Combinations of simulated scenarios of sea-level and storm surges. These were repeated for different durations (48 hours, 72 hours and 120 hours), with and without vegetation, for different timing of the storm surge with respect to tidal level (peak of the surge corresponding with HT or LT peak) and for different tidal ranges (surge occurring during spring or neap tide).

Tidal asymmetry has been recognised as one of the main factors controlling the net import/export of sediments and the large-scale morphological evolution of estuaries (Guo et al., 2016; Leonardi and Plater, 2017; Palazzoli et al., 2020) and there is evidence that changes in water level affect the tidal signal (Parker, 2007). It has been observed that, in shallow water, wind generated storm surges with period longer than the tidal period can cause an increase in water depth (when water level is raised by an onshore wind) and change the tidal dynamics by increasing the tidal range, causing a non-linear tidal distortion affecting the asymmetric non-linear terms that involve elevation for the period of the surge duration (Parker, 2007). Parker et al. (2007) suggests that these changes in the non-linear terms modify the harmonic constants since a greater tidal range leads to a maximum wave propagation velocity and minimum attenuation at crest and the opposite at through, causing an asymmetric distortion of the tide and generating second harmonics (e.g. M4). Sea-level is also known to cause modifications of the harmonic constants, as it causes changes in reflection and resonance of the tidal signal (van Maanen et al., 2013). To investigate the effect of storm surges and sea-level on the tidal signal, Fourier analysis was conducted for each scenario; changes in the tidal signal discussed for storm surge scenarios refer to time-limited modifications occurring during the period of the storm, while for sea-level scenarios the whole month was analysed. The MATLAB

package T-TIDE was used to conduct the analysis (Pawlowicz et al., 2002); for storm surges, the 48 hours scenarios occurring during spring tide was used for this purpose. The distortion and asymmetry of the tidal signal were analysed using the principal lunar semi-diurnal constituent M2 and the largest shallow water constituent M4; the distortion was calculated using the ratio $A_{4-2}=A_{M4}/A_{M2}$ where A is the amplitude of the tidal height and the asymmetry was calculated using $\Delta\theta=2\theta_{M2}-\theta_{M4}$ where θ is the phase of the tidal height (Friedrichs and Aubrey, 1988; Blanton et al., 2002). When $\Delta\theta$ is between 0° and 180° the flood phase dominates, whereas when it is between 180° and 360° the ebb phase dominates; the magnitude of A_{4-2} is representative of the significance of the dominance (Friedrichs and Aubrey, 1988). The harmonic analysis was not performed on dry cells and on salt marsh or tidal flat cells intermittently covered by water.

4. Results

4.1 Sediment budget

Figure 3 shows that for spring tide scenarios the cumulative sediment deposition increases overall in both the restricted domain and on the marsh platform when the surge height increases. For the 48 hours scenario, in the restricted domain, for higher surges, deposition is more substantial when the peak of the surge coincides with the high tide peak. On the marsh platform, the rise is more pronounced when the peak of the surge coincides with the low tide peak. For longer durations (72 hours and 120 hours scenarios), this difference decreases visibly and becomes negligible. Similarly, these trends remain comparable when a decrease in tidal range is applied (i.e. neap tide scenarios), but the difference between deposition driven by surges peaking at high tide and surges peaking at low tide becomes less significant (Figure 2 in Pannozzo et al., 2021). For all durations at spring tide (Figure 3), when vegetation is added, the trends show a variation both in the restricted domain and on the marsh. In the restricted domain, the deposition in the vegetated scenario is greater than the hypothetical non-vegetated scenario for surges up to 2 m and lesser for surges >2 m. Conversely, on the saltmarsh, the deposition in the vegetated scenario is lesser for surges up to 1 m and greater for

surges >1 m compared to the non-vegetated scenario. For neap tide scenarios (Figure 2 in Pannozzo et al., 2021), this inversion in the trends does not occur or it only occurs for surges >3 m. With an increase in sea-level (Figure 4), the cumulative sediment deposition decreases both in the restricted domain and on the marsh. When vegetation is added, no significant difference is noticeable in the trend.

When the surge and sea-level scenarios are combined, the trends in deposition caused by the increase in surge height remain similar in all sea-level scenarios (Figure 5). The main visible difference is a decrease in the difference between deposition during surges occurring at low tide and high tide in the restricted domain (Figure 5a), whereas on the marsh the difference increases (Figure 5b). However, there is an overall decrease in the magnitude of deposition with the increase in sea-level. Overall, it seems that the effects of storm surges mask the effects of sea-level rise on the sediment budget, both in the restricted domain and on the marsh platform; this is especially true for surges with the highest intensities (>3 m).

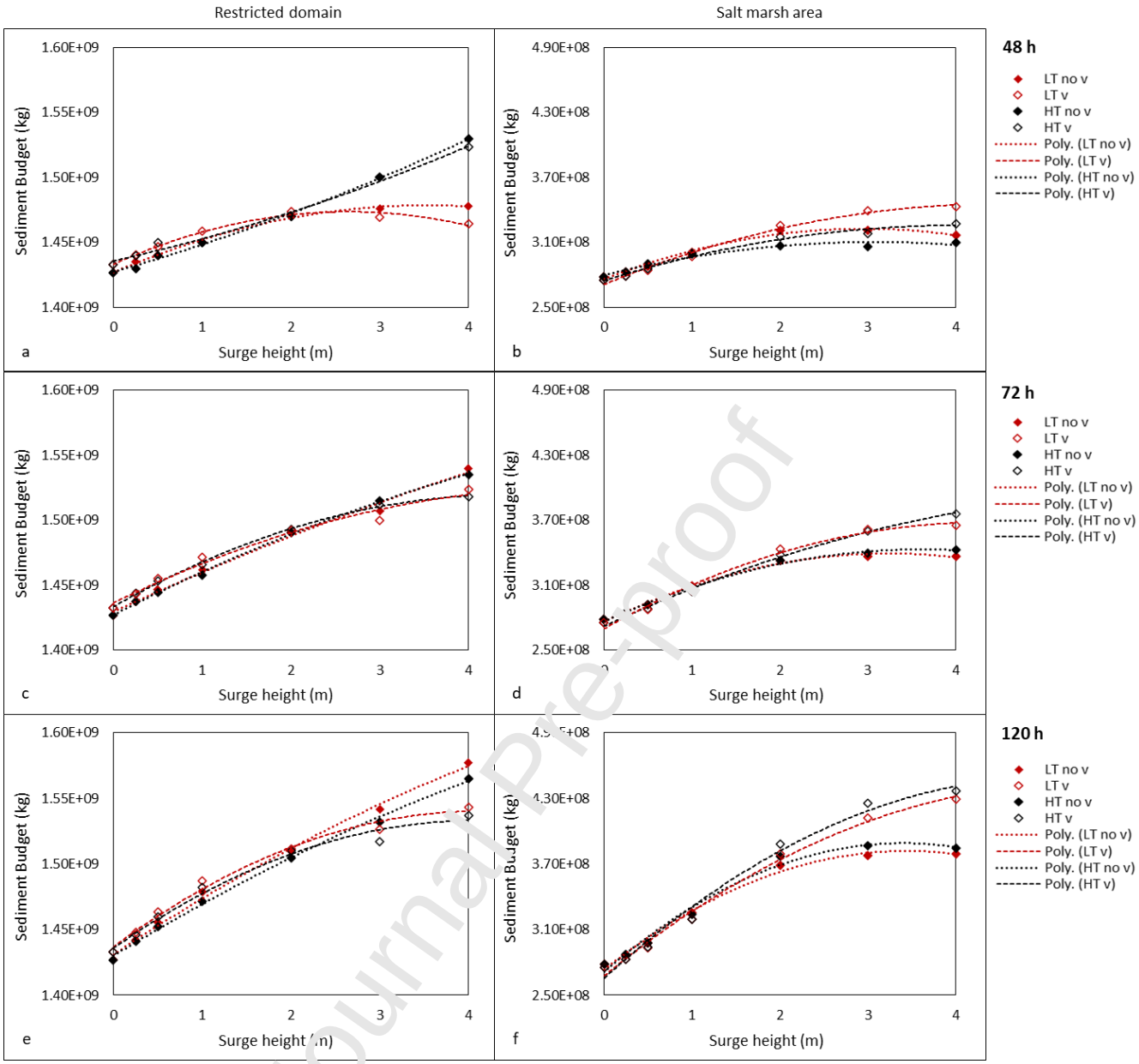

Figure 3. Sediment budget integrated across the entire area of the restricted domain (a, c, e) and the saltmarsh (b, d, f) for each surge height, for surges occurring at high tide (HT) and low tide (LT) without vegetation (no v) and with vegetation (v), for surges of different durations occurring at spring tide (see Figure 2 in Pannozzo et al., 2021 for surges occurring at neap tide); scenarios run using an ideal only-mud bed composition.

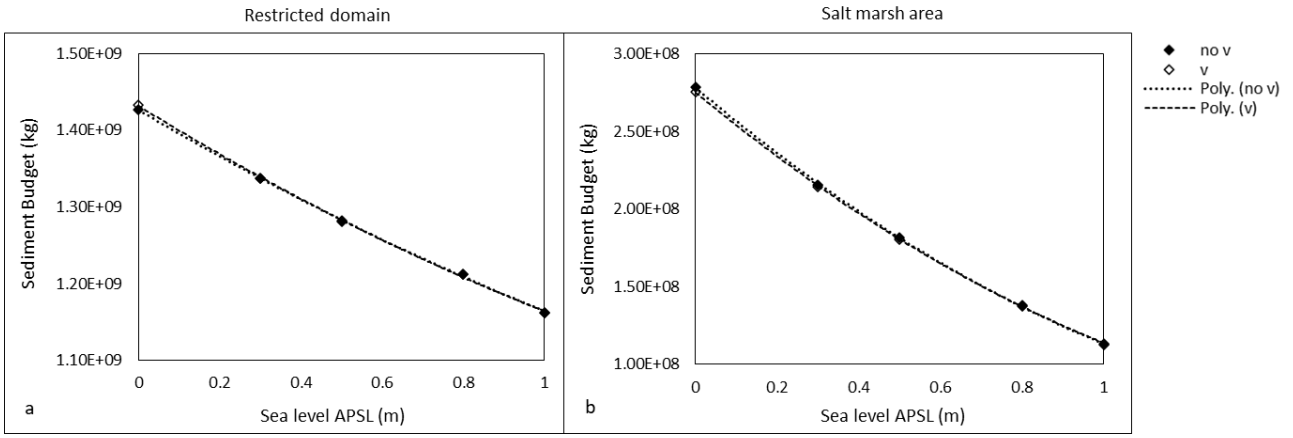

Figure 4. Sediment budget integrated across the entire area of the restricted domain (a) and the saltmarsh (b) for each sea-level scenario, without vegetation (no v) and with vegetation (v); scenarios run using an ideal only-mud bed composition.

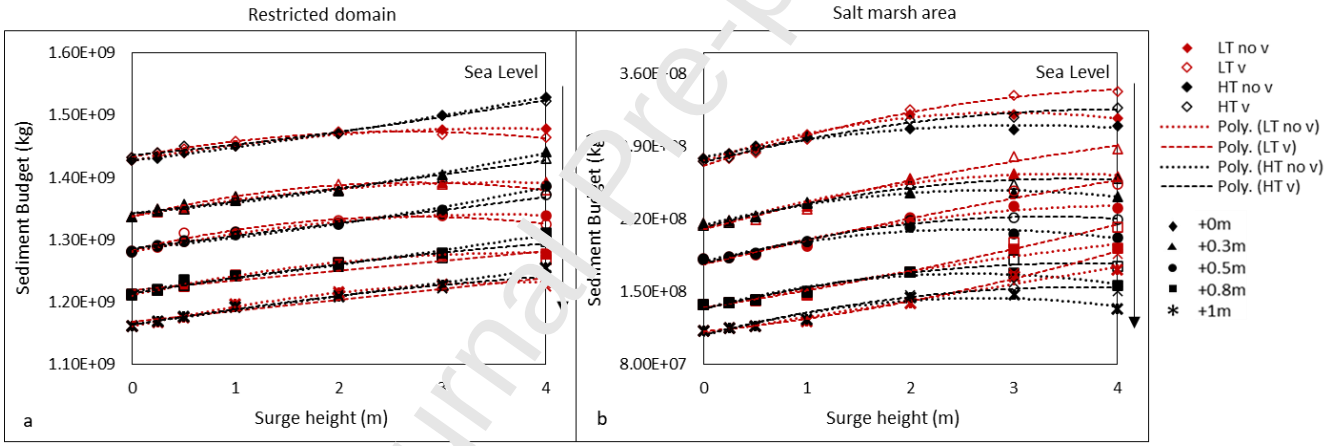

Figure 5. Sediment budget integrated across the entire area of the restricted domain (a) and the saltmarsh (b) for each combination of surge height and sea-level scenarios, for surges occurring at high tide (HT) and low tide (LT) without vegetation (no v) and with vegetation (v); scenarios run using an ideal only-mud bed composition. The analysis was performed using the 48 hours scenarios occurring at spring tide.

4.2 Tidal analysis

At present-day sea-level and no surges, the estuary is characterised by a dominance of the flood phase (Figure 6). Flood dominance decreases landward, accompanied by an initial increase in

distortion, as tides move from the deeper to the shallower portion of the estuary, which then reduces again around the shallower tidal flat areas (Figure 6). The overall flood dominance explains the positive sediment budget characterizing the system in a no sea-level rise and no surge scenario.

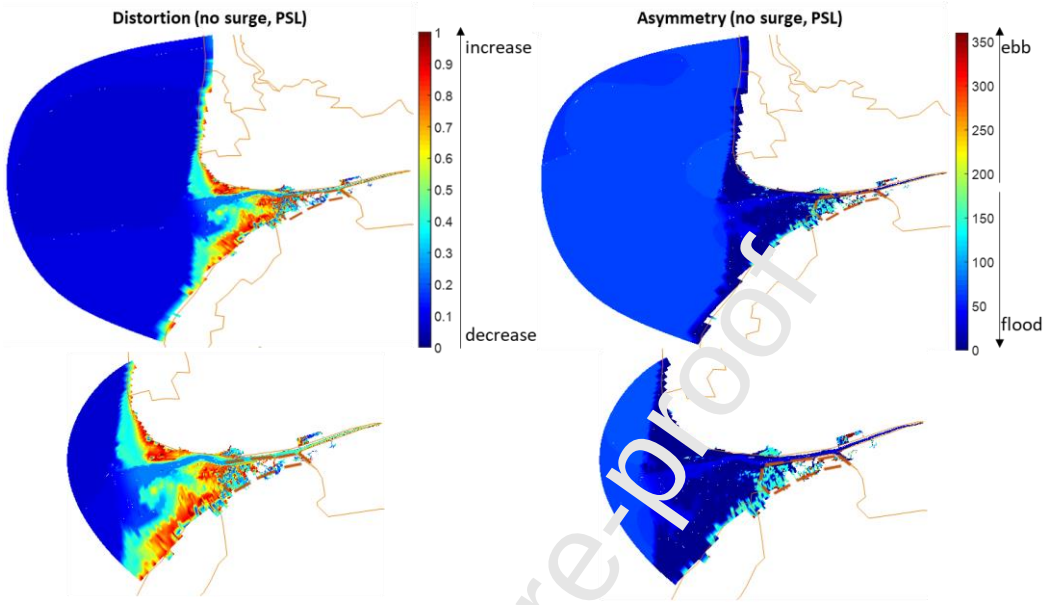

Figure 6. Tidal distortion (A_{4-2}) and asymmetry ($\Delta\theta$) at present sea-level (PSL) with no surges. Entire domain above and zoom on the inner estuary and tidal flat areas below. When $\Delta\theta$ is between 0° and 180° the flood phase dominates, when it is between 180° and 360° the ebb phase dominates; when the magnitude of A_{4-2} increases, the degree of the asymmetry is more significant and vice versa. The continuous brown lines correspond to the land boundary. The area enclosed by the brown dashed lines is the salt marsh.

In the presence of storm surges and for locations near the coastline (Figure 1, S1), the flood dominance and tidal distortion are strongly enhanced as the surge height increases (Figures 7 and 8). Conversely, further away from the coast (Figure 1, S2), the tidal signal is characterised by a reduction in distortion and a slight shift towards ebb dominance (Figures 7 and 8). The significant increase in distortion and flood dominance explains the increase in sediment deposition in the system seen in Figures 3 (above) and in Figure 2 from Pannozzo et al. (2021). The ebb shift offshore is slightly more pronounced when the surge occurs at low tide peak for higher surges

(Figure 7). This can explain the differences in deposition between surges occurring at high and low tide peak seen in the 48 hours scenarios at spring tide for the restricted domain (Figure 3a). On the salt marsh, for the same scenarios, the higher deposit caused by the surges occurring at low tide, compared to the surges occurring at high tide (Figure 3b), is likely to depend on the duration of the flooding, since in the first case the surge covers two high tide peaks, enhancing two flood events, whereas in the second case the surge covers only one high tide peak, enhancing only one flood event (Figures 2a and 2b). This difference becomes negligible for longer durations (Figure 3 c, d, e, f), since the number of tidal cycles covered by the surge increases enough to reduce the effect of the tidal harmonic on the amplification of the surge and the influence of surge timing. The same principle is applied for lower tidal ranges (i.e. neap tide scenarios, Figure S1); with a decrease in the amplitude of the tidal harmonic, there is a consequent reduction in the surge amplification.

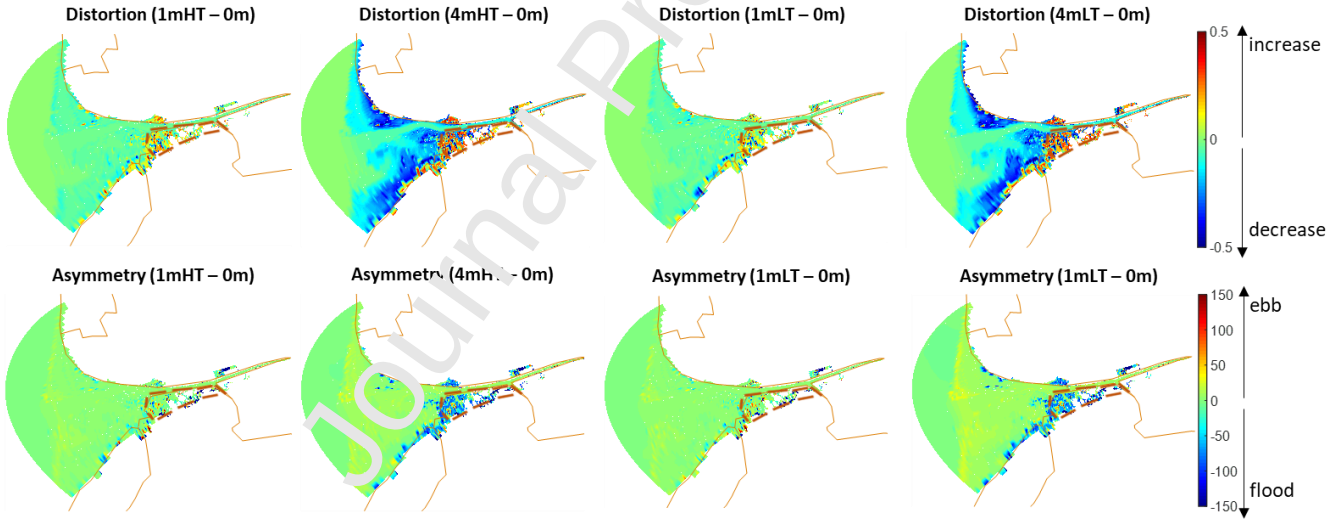

Figure 7. Difference between tidal distortion (A_{4-2}) and asymmetry ($\Delta\theta$) of 1 m and 4 m surge scenarios and the no surge scenario at current sea-level (see Figure 3 from Pannozzo et al., 2021 for the rest of the surge scenarios). When $\Delta\theta$ is positive there is an increase in ebb dominance with respect to the no surge scenario, when it is negative there is an increase in flood dominance; when A_{4-2} is positive, the degree of the asymmetry is more significant, vice versa when it is negative. The analysis was performed using the 48 hours scenarios occurring during spring tide. The continuous

brown lines correspond to the land boundary. The area enclosed by the brown dashed lines is the salt marsh.

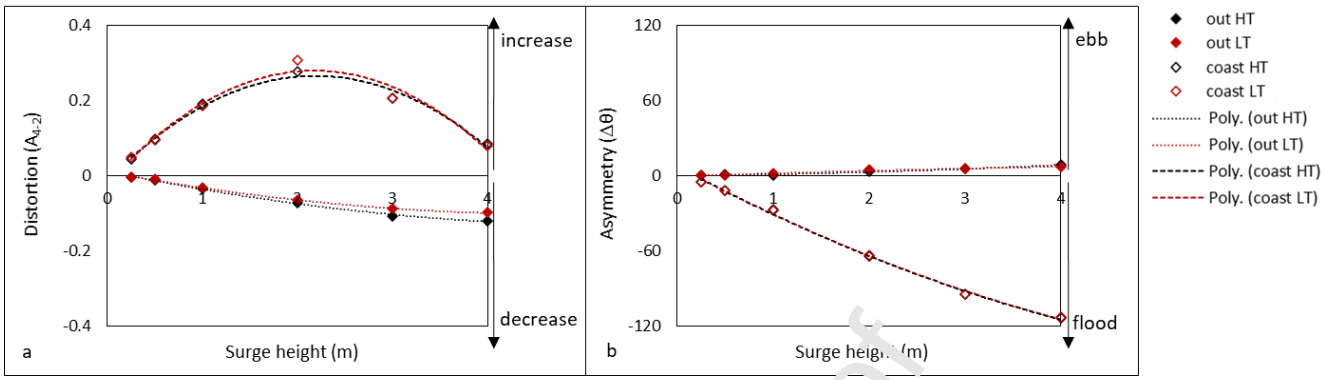

Figure 8. Difference between tidal distortion (A_{4-2}) (a) and asymmetry ($\Delta\theta$) (b) of all surge scenarios and the no surge scenario at current sea-level for one point along the coastline (coast) 53.64° N -3.02° E (Figure 1, S1) and one further away from the coast (out) 53.73° N -3.03° E (Figure 1, S2). When $\Delta\theta$ is positive there is an increase in ebb dominance with respect to the no surge scenario, when it is negative there is an increase in flood dominance; when A_{4-2} is positive, the degree of the asymmetry is more significant, vice versa when it is negative. The analysis was performed using the 48 hours scenarios occurring during spring tide.

When different sea-level scenarios are applied, as sea-level rises, locations near the coastline are characterised by an increasing ebb dominance (Figure 1, S3), which seems to be more significant on the deeper areas of the tidal flats, while it becomes less significant on the shallower areas of the tidal flats, where distortion decreases (Figures 9 and 10). This increase in ebb dominance explains the decrease in sediment deposition seen in the system in Figure 4. Conversely, further away from the coast (Figure 1, S4) an increase in distortion is associated to a strengthening of the flood dominance (Figures 9 and 10). The difference in deposition between surges occurring at high and low tide peak seen in the restricted domain for the 48 hours scenario at spring tide (Figure 3a) decreases with sea-level rise (Figure 5a); this can be explained by the offshore increase in flood dominance caused by sea-level rise (Figure 9) offsetting the difference in ebb dominance between

surges occurring at high tide peak and surges occurring at low tide peak (Figure 7). For the same scenarios, the difference in deposition between surges occurring at low tide peak and surges occurring at high tide peak on the marsh (Figure 3b) increases with sea-level rise, since greater water depth enhances inundation for two high tide peaks in the first case but only one high tide peak in the second case (Figures 2a and 2b). Overall, the impact of increasing storm surge heights on distortion and asymmetry is higher near the coastline (Figure 8), while the effect of sea-level rise is more pronounced in the outer estuary (Figure 10).

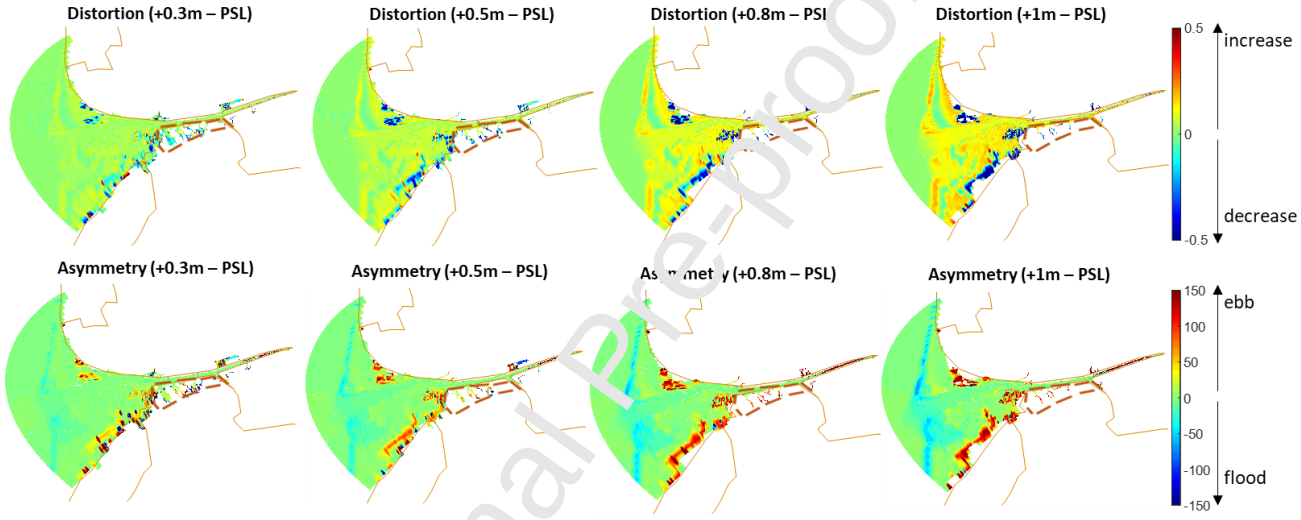

Figure 9. Difference between tidal distortion (A_{4-2}) and asymmetry ($\Delta\theta$) of all sea-level scenarios and the current sea-level scenario. When $\Delta\theta$ is positive there is an increase in ebb dominance with respect to the present sea-level scenario, when it is negative there is an increase in flood dominance; when A_{4-2} is positive, the degree of the asymmetry is more significant, vice versa when it is negative. The continuous brown lines correspond to the land boundary. The area enclosed by the brown dashed lines is the salt marsh.

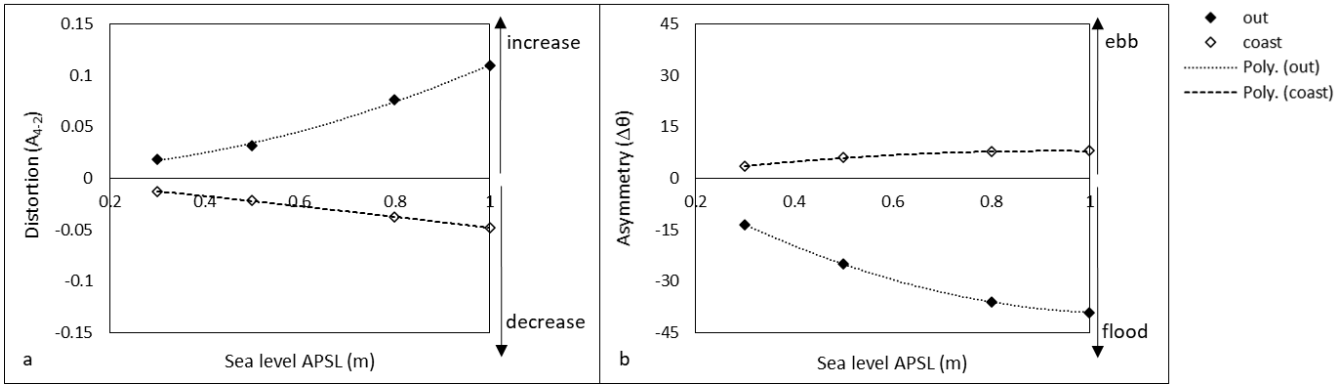

Figure 10. Difference between tidal distortion (A_{4-2}) (a) and asymmetry ($\Delta\theta$) (b) of all sea-level scenarios and the current sea-level scenario for one point along the coastline (coast) 53.63° N -3.06° E (Figure 1, S3) and one further away from the coast (out, 53.72° N -3.07° E (Figure 1, S4). When $\Delta\theta$ is positive there is an increase in ebb dominance with respect to the present sea level scenario, when it is negative there is an increase in flood dominance; when A_{4-2} is positive, the degree of the asymmetry is more significant, vice versa when it is negative.

4.3 Vegetation effect in storm surge scenarios

When vegetation is added, there is a change in current velocities in comparison to the hypothetical non-vegetated scenarios (Figure 11). In the spring tide scenarios, for the no surge scenario and for surges up to 1 m, as the surge height increases, on the marsh platform there is a consistent increase in flood velocity within the tidal creeks, whereas along the edge of the marsh there is a consistent decrease. This favours resuspension within the marsh area and deposition in the periphery, therefore leading to less deposition on the marsh platform but more in the restricted domain. During higher surges, the marsh platform is mainly characterised by lower velocities, whereas in the peripheric areas the higher velocities dominate. This favours deposition on the marsh area and excavation in the periphery, leading to more deposition on the marsh platform but less in the restricted domain. For the neap tide scenarios, this inversion does not occur at all or it only occurs for surges >3 m (Figure 2 in Pannozzo et al., 2021). During neap tide, the water level is lower during flood phase,

when the marsh is inundated, therefore the velocity profile typical of lower water depths persists for higher surges.

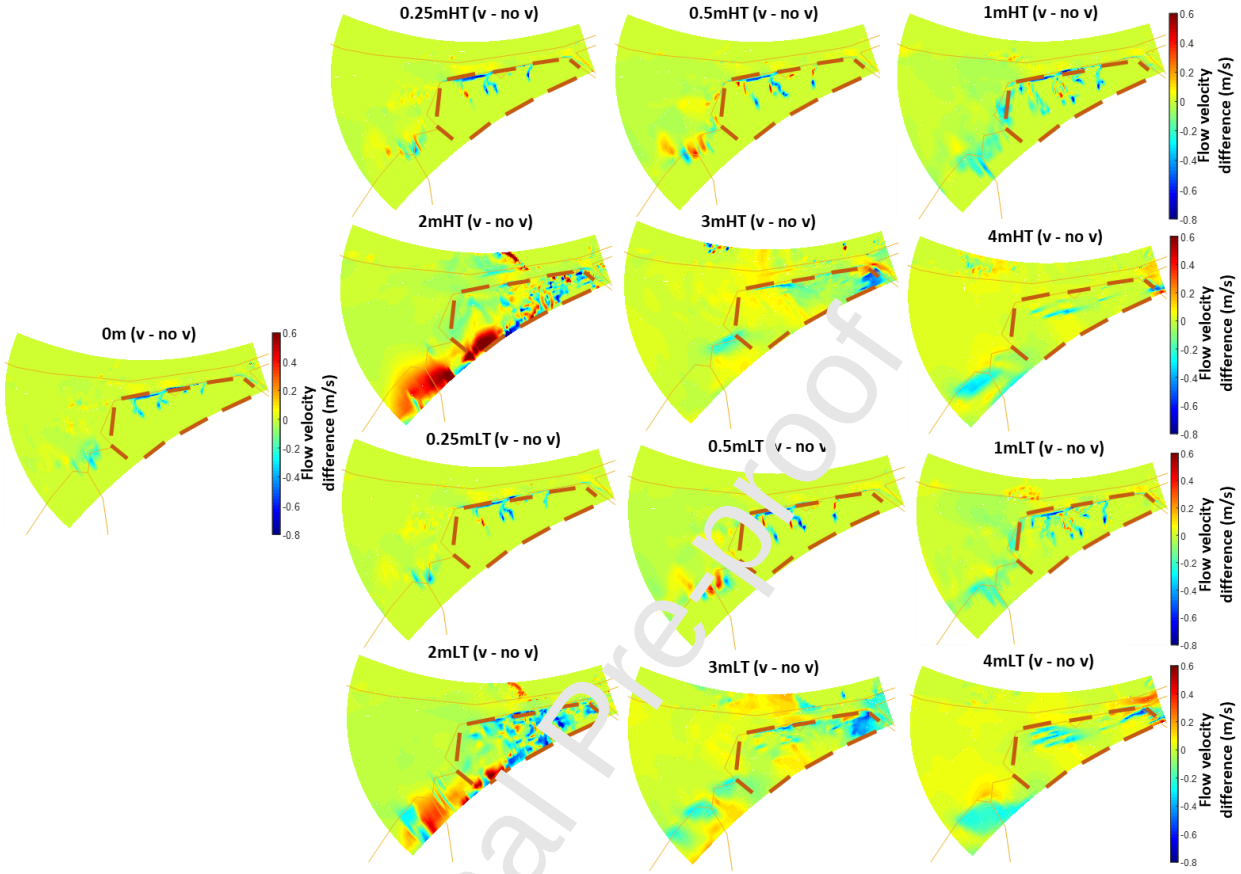

Figure 11. Difference between maximum current velocity during flood phase of vegetated (v) and hypothetical non-vegetated (no v) scenarios for all surge scenarios. The analysis was performed using the 48 hours scenarios occurring at spring tide. The continuous brown lines correspond to the land boundary. The area enclosed by the brown dashed lines is the salt marsh.

5. Discussion

The sediment budget of estuaries and saltmarshes depends on the quantity of sediment entering and exiting the system during each tidal cycle, and this is influenced by tidal asymmetry and distortion (Guo et al., 2016; Palazzoli et al., 2020). When there is a flood dominance (flood phase shorter and more intense than ebb phase), flood velocities can be sufficiently high to resuspend sediment and

promote a net landward sediment import, and vice versa in the case of ebb dominance (Van Dongeren and de Vriend, 1994; Lanzoni and Seminara, 2002).

For a no-sea-level rise and no-surge scenario, the system is overall flood dominated (Figure 6) with a positive sediment budget both in the restricted domain and on the marsh platform (Figure 3). The flood dominance significantly decreases for shallower tidal flats and marsh areas. This decrease is likely to be caused by a landward increase in friction, which reduces the velocity of the incoming tide (Friedrichs and Aubrey, 1988; Wang et al., 2002; Parker, 2007). This phenomenon has been observed in some of the major estuaries around the world, where the friction effect is dominant in the upper estuary – e.g. the Severn Estuary in UK (Lyddon et al., 2018) and the Westerschelde estuary in the Netherlands (Wang et al., 2002).

5.1 Storm surges

Storm surge presence enhances the flood dominance near the coastline and causes a slight ebb dominance offshore (Figures 7 and 8, Figure 3 from Pannozzo et al., 2021). The most important term affecting the non-linear interaction between storm surges and tides in shallow water is the non-linear bottom friction term (Zengrao and Yihong, 1996; Parker, 2007). When a storm surge causes an increase in water level and has period longer than the tidal period, the water depth increases due to the effect of the surge, reducing the bottom friction (Figure 4) and, therefore, increasing the propagation speed of the tidal wave which is depth dependent (Rossiter, 1961; Wolf, 1981; Parker, 2007). This leads to an increase in the speed of the flood phase, as the crest of the tide partially overtakes the trough; hence the enhancement of flood dominance near the coastline caused by the increase in surge height (Friedrichs and Aubrey, 1988; Olbert, 2013). The non-linear interaction between tide and storm surge has been well observed for several years (eg. Rossiter, 1961; Wolf, 1981; Parker, 1991). For instance, Parker (1991) described a tidal signal several locations along Delaware Bay (USA) with shorter and faster flood phase compared to the predicted signal during the occurrence of a subtidal storm surge.

In deeper water, where the effect of the bottom friction is less prevalent, the symmetric relationship of tide and velocity might be the dominant factor that controls the phase dominance (Savenije, 2012). Therefore, the increase in water level caused by the increase in surge height could be responsible for the offshore increase in ebb dominance (Wang et al., 2002; Moore et al., 2009). This is, for instance, observed in the Dee Estuary (UK) where the tidal flats are mainly characterised by a distorted flood dominated tidal signal, while in the deeper channel the signal is less distorted and the ebb phase results to be dominant (Moore et al., 2009). This also explains the more pronounced offshore ebb dominance when the surge peaks at low tide compared to when it peaks at high tide (as observed for the 48 hours scenarios at spring tide but not for the longer durations or the reduced tidal range). In the first case the surge covers two high tide peaks, therefore, the ebb phase offshore is enhanced two times, whereas in the second case the surge covers only one high tide peak, enhancing the ebb phase only once (Figures 2a and 2b), but as the number of tidal cycles increases or the amplitude of the tidal signal decreases, the amplification of this effect is reduced. This reduced differences between deposition produced by surges occurring at high tide and surges occurring at low tide peak has been observed in microtidal regimes. This is the case of most US Atlantic bays where the tidal range is about 20 cm - e.g., Virginia Bay (Castagno et al., 2018). The results of this study show that, overall, storm surges contribute to make the salt marsh and estuarine system more resilient, in agreement with other studies (Turner et al., 2006; Walters and Kirwan, 2016; Castagno et al., 2018).

5.2 Sea-level

An increase in sea-level causes ebb dominance near the coastline and enhanced flood dominance offshore (Figures 9 and 10). The increase in water level caused by sea-level rise is responsible for an increase in the tidal prism (i.e. volume of the water flowing into the estuary) which in turn causes an increase in the velocity of the incoming tide across the mouth of the estuary (Sinha et al., 1997; Liu et al., 2020; Zhang et al., 2020); this can explain the enhanced flood dominance offshore.

Several estuaries around the world have shown a similar behaviour. For example, this phenomenon has been found to be responsible for a decrease in ebb dominance in the whole estuarine system and consequent rejuvenation of the Tairua Estuary, New Zealand (Liu et al., 2020).

However, in the nearshore, the estuary becomes more ebb dominated as sea-level rises (Figures 9 and 10). The Irish Sea, where the Ribble Estuary is located, is influenced by a phenomenon of resonance, and it has been shown that an increase in sea-level can produce changes in resonance properties that are negligible in deep water but can be observed in shallow water (Pugh, 1987). Several studies have been conducted on the effect of sea-level rise on tidal constituents in the European Shelf, including the Irish Sea, and they showed that a rise in sea-level affects the resonance of the basin causing an increase in the M2 component (Pickering et al., 2012; Idier et al., 2017). This could be responsible for the ebb dominance that characterises the inner estuary and the tidal flat areas. Other estuaries on the European Shelf have been found to behave in the same way e.g. the Bristol Channel in UK and the Gulf of St. Malo in France (Pickering et al., 2012; Idier et al., 2017).

This study showed that sea-level rise might threaten the stability of the salt marsh, in agreement with the results of previous studies (FitzGerald et al., 2008; Kirwan et al., 2010; Ganju et al., 2017). Nevertheless, the data presented here show that storms have a general tendency to increase marsh resilience to sea-level rise by counteracting the decrease in sediment budget caused by sea-level rise (Figure 5). This is particularly true for storms with the highest intensity (>3 m surges), in agreement with Schuerch et al. (2013). In terms of relative contribution, Figure 5 shows that, on the marsh platform, storm surges of 48 hours occurring at spring tide can cause up to 65% reduction in sediment loss driven by sea-level rise; in the restricted domain this reduction can reach 7%. Trends in Figure 3 suggest that an increase in duration could amplify this reduction, while Figure S1 shows that a decrease in tidal range could minimize it. Wang et al. (2020) found that a similar level of contribution is provided by storms to the resilience of deltas experiencing erosion driven by high

river discharge; here they help reducing the sediment loss induced by riverine flows by over 50%. It is, however, significant to highlight that storm surges with height up to 2 m have substantially lower return period (between 2 and 100 years), while surges >3 m are much less frequent (between 100 years and 1000 years return period) (see Table 1 in Pannozzo et al., 2021). This suggests that the effects related to the surges of height up to 2 m have greater probability to be detected in reality, while the effects of >3 m surges are rarer to observe.

5.3 Vegetation effect

The addition of vegetation does not significantly modify the trends of deposition caused by the storm surges and the increase in sea-level. However, it causes minor changes in the deposit of different storm surge scenarios (Figure 3). Vegetation enhances sediment deposition trough particle capture by plant stems and enhanced particle settling caused by a reduction in turbulent kinetic energy of the water flow through the plant canopy (Neumeier and Ciavola, 2004; Mudd et al., 2010). However, it also affects sediment deposition indirectly by channelizing water and increasing flood velocity within tidal creeks and off site, favouring excavation (Temmermann et al., 2005).

In the spring tide scenarios, for the no surge scenario and for surges up to 1 m, when vegetation is present, the water level is not high enough to overflow the tidal creeks since the vegetation on the marsh platform acts as a barrier (Figure 5 in Pannozzo et al., 2021); this enhances the velocities of the incoming tide, causing excavation and preventing deposition, hence, there is lower deposition on the marsh platform compared to the hypothetical non-vegetated scenarios (Figure 3 b, d, f). Along the edge of the marsh, where the water is not constrained (Figure 5 in Pannozzo et al., 2021), the frictional effect of the vegetation causes a decrease in velocity (Figure 11), favouring particle settling on the periphery of the marsh, hence, the higher deposition in the restricted domain compared to the non-vegetated scenarios (Figure 3 a, c, e). During higher surges, the water level is high enough to overflow the tidal creeks despite vegetation (Figure 5 in Pannozzo et al., 2021), therefore the vegetation present on the marsh platform enhances particle settling, as showed by the

dominance of the lower velocities (Figure 11), leading to sediment deposition being higher in vegetated scenarios (Figure 3 b, d, f). Outside the tidal flat areas, the higher velocities dominate (Figure 11). The frictional effect of the vegetation might not be effective on the high-water depths on the edge of the marsh (Beudin et al., 2017), whereas the off-site water channelization might dominate, causing excavation. Therefore, leading to less deposition in the restricted domain compared to the non-vegetated scenarios (Figure 3 a, c, e). The neap tide scenarios show similar trends (Figure 2 in Pannozzo et al., 2021), but the inversion does not occur at all or it only occurs for surges >3 m. During neap tide, the water level is lower during flood phase, when the marsh is inundated, therefore the channelling effect caused by vegetation on the marsh platform persists for higher surges. In the rest of the domain, where water is not channelised, the water level remains low enough to allow particle settling on the periphery of the marsh, even for greater surges.

With a rise in sea-level, there is no difference in the sediment budget between the vegetated and the hypothetical non-vegetated scenario. Sea-level rise produces an increase in water depth (Figure 2c). This increase leads to a rise in water level in the tidal creeks and along the edge of the marsh, during flood phase, which produces water depth profiles similar to the ones observed for surges up to 1 m (Figure 5 in Pannozzo et al., 2021). However, since storm surges trigger a net import of sediment, the quantity of suspended sediment in the system during these events is high enough to allow vegetation to contribute towards accretion/erosion of the different areas of the marsh platform. Conversely, sea-level rise is responsible for sediment export, therefore with sea-level higher than present day the quantity of suspended sediment in the system is never high enough to allow a contribution by vegetation that can be easily observed in the trends.

Overall, when an interaction between the tidal channels and the marsh platform is considered (Temmerman et al., 20005; D'Alpaos et al., 2007; Kirwan and Murray, 2007), vegetation does not seem to significantly affect the trends, and this agrees with the observations of Li et al. (2018).

5.4 Further considerations

The period used for this study is January 2008. However, it is worthwhile to consider that the ultimate sediment budget can change slightly depending on the period of the year considered and the relative river discharge. The river flow, which is in the direction of the tidal current during ebb phase and in its opposite direction during flood phase, causes a bottom friction effect and non-linearly interacts with the tide, enhancing ebb velocities and reducing flood velocities (Parker, 2007). During flood periods, when river discharge increases, this effect is enhanced, promoting more sediment export (Parker, 1984).

The Ribble Estuary experiences moderate wave energy (Pye and Neal, 1994). However, for simplicity, the effects of wind waves have been neglected in this study to define the distinct effects of surges and sea-level. Even though several studies have shown that storm waves can contribute to marsh erosion (Marani et al., 2011; Fagherazzi et al., 2013; Leonardi and Fagherazzi, 2014; Leonardi et al., 2016; Li et al., 2019), others have also shown that wind waves can resuspend sediments from the seabed, which can then be transported into the estuarine system by tidal currents, contributing to deposition (Fernández-Mora et al., 2015; Brooks et al., 2017) and potentially supporting marsh maintenance. The effect of wind waves in the scenarios analysed above will be investigated in further studies.

Finally, it must be considered that in this manuscript the effects of sea-level rise and storm surges were analysed by looking at the response of sediment fluxes to changing hydrodynamic forcing over a timescale of 30 days. In reality, changes in sea-level would occur within the time scale of decades to century during which salt marshes can undergo intrinsic morphological transformations. Salt marshes adapt to hydrodynamic changes, such as sea-level rise, in a timeframe of c.a. 10-100 years (e.g., Kirwan and Murray, 2008; D'Alpaos et al., 2011), while sediment delivered by storm surge events are deposited instantaneously on the marsh platform, allowing marshes to rapidly accrete by steps (e.g., Schuerch et al., 2018). This suggests that the offsetting of sea-level rise effects on the sediment budget caused by storm surges might be even more amplified in reality.

6. Conclusions

This study investigated the resilience of salt marshes to the combined influence of sea-level rise and increasing storm surge intensity on the sediment budget of a salt marsh-tidal flat complex using a numerical model of the Ribble Estuary, North-West England. Different storm surges and sea-level rise magnitudes were simulated and the influence of storm duration and local factors (i.e. the timing of occurrence of the surge with respect to tidal levels, tidal range and vegetation) on the nature and amplitude of changes in sediment budget were also considered. The study concluded that storm surges could contribute to salt marsh and estuarine resilience by causing a shift towards a more flood dominated system and by triggering a net import of sediment. The degree of deposition can change slightly depending on the timing of the surge peak for short durations (48 hours) and high tidal range, while it is reduced if the duration increases (72 hours and 120 hours) or the tidal range decreases. Conversely, sea-level rise will threaten the stability of the marsh by causing a shift towards an ebb dominated system, triggering a higher export of sediment. It seems that storm surges might contribute to increase saltmarsh resilience to sea-level rise by masking the effects of sea-level rise on the sediment budget; this is particularly true for storms with highest intensities (>3 m surges). The sediment loss driven by sea-level rise can be reduced by up to 65% on the marsh platform and by up to 7% in the restricted domain when surges occur at spring tide and last 48 hours, with further reduction when surge duration increases, but lower reduction when tidal range decreases. Nevertheless, since storm surges with height up to 2 m have a lower return period, the effects related to these surges have higher probability to be detected, while surges >3 m occur less frequently, meaning that their effects are rarer to observe. The addition of vegetation caused no variations to the trends produced by the sea-level analysis and only minimal variations to the trends produced by surge height analysis; the latter is due to the ability of vegetation canopy to modify flow velocity.

Acknowledgements

We acknowledge support from the School of Environmental Sciences, University of Liverpool which is funding the PhD project of the first Author. This model for the Ribble Estuary was originally designed as part of the projects 'Adaptation and Resilience of Coastal Energy Supply (ARCoES)' and 'Physical and biological dynamic coastal processes and their role in coastal recovery (BLUE-coast)' and we are grateful for being able to use the model. The model is also presented in Li et al., 2018, 2019. We thank two anonymous reviewers for their constructive feedback on the manuscript.

Data availability

Data related to this article can be found in the following repository: https://doi.org/10.5281/zenodo.4511397. Data are also described in Pannozzo et al., 2021 (Data in Biref).

References

Baptist, M.J., Babovic, V., Uthurburu, J.R., Keijzer, M., Uittenbogaard, R.E., Mynett, A., Verwey, A., 2007. On inducing equations for vegetation resistance. Journal of Hydraulic Research, 45 (4), 435-450. https://doi.org/10.1080/00221686.2007.9521778

Barbier, E.B., Hacker, S.D., Kennedy, C., Koch, E.W., Stier, A.C., Silliman, B.R., 2011. The value of estuarine and coastal ecosystem services. Ecological Monographs, 81 (2), 169-193. https://doi.org/10.1890/10-1510.1

Beudin, A., Kalra, T.S., Ganju, N.K., Warner, J.C., 2017. Development of a coupled wave-flow-vegetation interaction model. Computers & Geosciences, 100, 76-86. https://doi.org/10.1016/j.cageo.2016.12.010

Blanton, J.O., Lin, G.Q., Elston, S.A., 2002. Tidal current asymmetry in shallow estuaries and tidal creeks. Continental Shelf Research, 22 (11-13), 1731-1743. https://doi.org/10.1016/s0278-4343(02)00035-3

Brooks, S.M., Spencer, T., Christie E.K., 2017. Storm impacts and shoreline recovery: Mechanisms and controls in the southern North Sea. Geomorphology, 283: 48-60. https://doi.org/10.1016/j.geomorph.2017.01.007

Castagno, K.A., Jimenez-Robles, A.M., Donnelly, J.P., Wiberg, P.L., Fenster, M.S., Fagherazzi, S., 2018. Intense Storms Increase the Stability of Tidal Bays. Geophysical Research Letters, 45 (11), 5491-5500. https://doi.org/10.1029/2018gl078208

D'Alpaos, A., Lanzoni, S., Marani, M., Rinaldo A., 2007. Landscape evolution in tidal embayments: Modeling the interplay of erosion, sedimentation, and vegetation dynamics. Earth Surface, 112, F01008. https://doi.org/10.1029/2006JF000537

D'Alpaos, A., Mudd, S. M., Carniello L., 2011. Dynamic response of marshes to perturbations in suspended sediment concentrations and rates of relative sea level rise. Earth Surface, 116 (F24). https://doi.org/10.1029/2011JF002093

DELFT Hydraulics, 2014. Delft3D-FLOW User Manual: Simulation of multi-dimensional hydrodynamic flows and transport phenomena. https://oss.deltares.nl/documents/183920/185723/Delft3D-FLOW_User_Manual.pdf

Fagherazzi, S., Mariotti, G., Wiberg, P.L., McGlathery, K.J., 2013. Marsh Collapse Does Not Require Sea Level Rise. Oceanography, 26 (3), 70-77. https://doi.org/10.5670/oceanog.2013.47

Fernández-Mora, A., Calvete, D., Falqués, A., Swart H.E., 2015. Onshore sandbar migration in the surf zone: New insights into the wave-induced sediment transport mechanisms. Geophysical Research Letters, 42 (8): 2869-2877. https://doi.org/10.1002/ 2014GL063004

FitzGerald, D.M., Fenster, M.S., Argow, B.A., Buynevich, I.V., 2008. Coastal impacts due to sea-level rise. Annual Review of Earth and Planetary Sciences, 36, 601-647. https://doi.org/10.1146/annurev.earth.35.031306.140139

Friedrichs, C.T., Aubrey, D.G., 1988. NON LINEAR TIDAL DISTORTION IN SHALLOW WELL-MIXED ESTUARIES - A SYNTHESIS. Estuarine Coastal and Shelf Science, 27 (5), 521-545. https://doi.org/10.1016/0272-7714(88)90082-0

Ganju, N.K., Defne, Z., Kirwan, M.L., Fagherazzi, S., D'Alpaos, A., Carniello, L., 2017. Spatially integrative metrics reveal hidden vulnerability of microtidal salt marshes. Nature Communications, 8. https://doi.org/10.1038/ncomms14156

Ganju, N.K., Kirwan, M.L., Dickhudt, P.J., Guntenspergen, G.R., Cahoon, D.R., Kroeger, K.D., 2015. Sediment transport-based metrics of wetland stability. Geophysical Research Letters, 42 (19), 7992-8000. https://doi.org/10.1002/2015gl065980

Guo, L.C., van der Wegen, M., Wang, Z.B., Roelvink, D., He, Q., 2016. Exploring the impacts of multiple tidal constituents and varying river flow on long-term, large-scale estuarine morphodynamics by means of a 1-D model. Journal of Geophysical Research-Earth Surface, 121 (5), 1000-1022. https://doi.org/10.1002/2016jf003821

Idier, D., Paris, F., Le Cozannet, G., Boulahya, F., Dumas, F., 2017. Sea-level rise impacts on the tides of the European Shelf. Continental Shelf Research, 137, 56-71. https://doi.org/10.1016/j.csr.2017.01.007

Marani, M., D'Alpaos, A., Lanzoni, S., Santalucia, M., 2011. Understanding and predicting wave erosion of marsh edges. Hydrology and Land Surface Studies, 38 (21), L21401. https://doi.org/10.1029/2011GL048995

Masson-Delmotte, V., Zhai, P., Pörtner, H.-O., Roberts, D., Skea, J., Shukla, P.R., Pirani, A., Moufouma-Okia, W., Péan, C., Pidcock, R., Connors, S., Matthews, J.B.R., Chen, Y., Zhou,

X., Gomis, M.I., Lonnoy, E., Maycock, T., Tignor M., Waterfield T., 2018. Summary for Policymakers. In: Global Warming of 1.5°C. An IPCC Special Report on the impacts of global warming of 1.5°C above pre-industrial levels and related global greenhouse gas emission pathways, in the context of strengthening the global response to the threat of climate change, sustainable development, and efforts to eradicate poverty. In Press. https://www.ipcc.ch/2018/10/08/summary-for-policymakers-of-ipcc-special-report-on-global-warming-of-1-5c-approved-by-governments/

Kirwan, M.L., Guntenspergen, G.R., D'Alpaos, A., Morris, J.T., Mudd, S.M., Temmerman, S., 2010. Limits on the adaptability of coastal marshes to rising sea level. Geophysical Research Letters, 37. https://doi.org/10.1029/2010gl045489

Kirwan, M.L., Murray A.B., 2007. A coupled geomorphic and ecological model of tidal marsh evolution. PNAS, 104, 15, 6118-6122. https://doi.org/10.1073/pnas.0700958104

Kirwan, M. L., Murray A. B., 2008. Tidal marshes as disequilibrium landscapes? Lags between morphology and Holocene sea level change. Geophysical Research Letters, 34 (24), L24401. https://doi.org/10.1029/2008GL036050

Kirwan, M.L., Temmerman, S., Skeehan, E.E., Guntenspergen, G.R., Fagherazzi, S., 2016. Overestimation of marsh vulnerability to sea level rise. Nature Climate Change, 6 (3), 253-260. https://doi.org/10.1038/nclimate2909

Lanzoni, S., Seminara, G., 2002. Long-term evolution and morphodynamic equilibrium of tidal channels. Journal of Geophysical Research - Oceans, 107 (C1). https://doi.org/10.1029/2000jc000468

Leonardi, N., Carnacina, I., Donatelli, C., Ganju, N.K., Plater, A.J., Schuerch, M., Temmerman, S., 2018. Dynamic interactions between coastal storms and salt marshes: A review. Geomorphology, 301, 92-107. https://doi.org/10.1016/j.geomorph.2017.11.001

Leonardi, N., Fagherazzi, S., 2014. How waves shape salt marshes. Geology, 42 (10), 887-890. https://doi.org/10.1130/g35751.1

Leonardi, N., Ganju, N.K., Fagherazzi, S., 2016. A linear relationship between wave power and erosion determines salt-marsh resilience to violent storms and hurricanes. Proceedings of the National Academy of Sciences of the United States of America, 113 (1), 64-68. https://doi.org/10.1073/pnas.1510095112

Leonardi, N., Plater, A.J, 2017. Residual flow patterns and morphological changes along a macro- and meso-tidal coastline. Advances in Water Resources, 109, 290-301. https://doi.org/10.1016/j.advwatres.2017.09.013

Li, X.R., Leonardi, N., Plater, A.J, 2019. Wave-driven sediment resuspension and salt marsh frontal erosion alter the export of sediments from macro-tidal estuaries. Geomorphology, 325, 17-28. https://doi.org/10.1016/j.geomorph.2018.10.004

Li, X.R., Plater, A., Leonardi, N., 2018. Modelling the Transport and Export of Sediments in Macrotidal Estuaries with Eroding Salt Marsh. Estuaries and Coasts, 41 (6), 1551-1564. https://doi.org/10.1016/j.geomorph.2017.11.001

Liu, Z.C., de Lange, W.P., Bryan, K.R., 2020. Estuary rejuvenation in response to sea level rise: an example from Tairua Estuary, New Zealand. Geo-Marine Letters, 40 (2), 269-280. https://doi.org/10.1007/s00367-019-00603-0

Lyddon, C., Brown, J.M., Leonardi, N., Plater, A.J., 2018. Flood Hazard Assessment for a Hyper-Tidal Estuary as a Function of Tide-Surge-Morphology Interaction. Estuaries and Coasts, 41 (6), 1565-1586. https://doi.org/10.1007/s12237-018-0384-9

Lyons, M.G., 1997. The dynamics of suspended sediment transport in the Ribble estuary. Water Air and Soil Pollution, 99 (1-4), 141-148. https://doi.org/10.1023/a:1018388517409

Moller, I., Spencer, T., French, J.R., Leggett, D.J., Dixon, M., 1999. Wave transformation over salt marshes: A field and numerical modelling study from north Norfolk, England. Estuarine Coastal and Shelf Science, 49 (3), 411-426. https://doi.org/10.1006/ecss.1999.0509

Moore, R.D., Wolf, J., Souza, A.J., Flint, S.S., 2009. Morphological evolution of the Dee Estuary, Eastern Irish Sea, UK: A tidal asymmetry approach. Geomorphology, 103 (4), 588-596. https://doi.org/10.1016/j.geomorph.2008.08.003

Morris, J.T., Sundareshwar, P.V., Nietch, C.T., Kjerfve, B., Cahoon, D.R., 2002. Responses of coastal wetlands to rising sea level. Ecology, 83 (10), 2869-2877. https://doi.org/10.2307/3072022

Mudd, S.M., D'Alpaos, A., Morris, J.T., 2010. How does vegetation affect sedimentation on tidal marshes? Investigating particle capture and hydrodynamic controls on biologically mediated sedimentation. Journal of Geophysical Research-Earth Surface, 115. https://doi.org/10.1029/2009jf001566

Neumeier, U., Ciavola, P., 2004. Flow resistance and associated sedimentary processes in a Spartina maritima salt-marsh. Journal of Coastal Research, 20 (2), 435-447. https://doi.org/10.2112/1551-5036(2004)020[0435:fraasp]2.0.co;2

Olbert, A.I., Nash, S., Cunnane, C., Hartnett, M., 2013. Tide-surge interactions and their effects on total sea levels in Irish coastal waters. Ocean Dynamics, 63 (6), 599-614. https://doi.org/10.1007/s10236-013-0618-0

Palazzoli, I., Leonardi, N., Jimenez-Robles, A.M., Fagherazzi, S., 2020. Velocity skew controls the flushing of a tracer in a system of shallow bays with multiple inlets. Continental Shelf Research, 192. https://doi.org/10.1016/j.csr.2019.104008

Pannozzo, N., Leonardi, N., Carnacina, I., Smedley, R., 2021 Dataset of results from numerical simulations of increased storm intensity in an estuarine salt marsh system, Data in Brief, In Press.

Parker, B. B., 1984. Frictional Effect on the Tidal Dynamics of a Shallow Estuary. Ph.D. Dissertation, The Johns Hopkins University, Baltimore, Maryland, pp. 292.

Parker, B. B., 1991. The relative importance of the various nonlinear mechanisms in a wide range of tidal interactions. In: Tidal Hydrodynamics (pp. 237-268), New York: John Wiley & Sons.

Parker, B.B, 2007. Tidal analysis and prediction. Silver Spring, MD: NOAA NOS Center for Operational Oceanographic Products and Services. http://dx.doi.org/10.25607/OBP-191

Partheniades, E., 1965. Erosion and deposition of cohesive soils. Journal of the Hydraulics Division, 91 (1), 105–139. https://cedb.asce.org/CEDBsearch/record.jsp?dockey=0013640

Pawlowicz, R., Beardsley, B., Lentz, S., 2002. Classical tidal harmonic analysis including error estimates in MATLAB using T-TIDE. Computers & Geosciences, 28 (8), 929-937. https://doi.org/10.1016/s0098-3004(02)00013-4

Pickering, M.D., Wells, N.C., Horsburgh, K.J., Green, J.A.M., 2012. The impact of future sea-level rise on the European Shelf tides. Continental Shelf Research, 35, 1-15. https://doi.org/10.1016/j.csr.2011.11.011

Pugh, D., 1987. Tides, Surges and Mean Sea-Level. Chichester: John Wiley & Sons Ltd.

Pye, K., Neal, A., 1994. COASTAL DUNE EROSION AT FORMBY POINT, NORTH MERSEYSIDE, ENGLAND - CAUSES AND MECHANISMS. Marine Geology, 119 (1-2), 39-56. https://doi.org/10.1016/0025-3227(94)90132-2

Reed, D.J., 1990. THE IMPACT OF SEA-LEVEL RISE ON COASTAL SALT MARSHES. Progress in Physical Geography, 14 (4), 465-481. https://doi.org/10.1177/030913339001400402

Reed, D.J., 1995. THE RESPONSE OF COASTAL MARSHES TO SEA-LEVEL RISE - SURVIVAL OR SUBMERGENCE. Earth Surface Processes and Landforms, 20 (1), 39-48. https://doi.org/10.1002/esp.3290200105

Rossiter, J.R., 1961. INTERACTION BETWEEN TIDE AND SURGE IN THE THAMES. Geophysical Journal of the Royal Astronomical Society, 6 (1), 29-53. https://doi.org/10.1111/j.1365-246X.1961.tb02960.x

RSPB, 2019. Hesketh Out Marsh, Ribble Estuary Nature Reserve - The RSPB. https://www.rspb.org.uk/

Savenije, H.H.G., 2012. Salinity and Tides in Alluvial Estuaries. Second Completely Revised Edition. Elsevier Science Ltd. https://hubertsavenije.files.wordpress.com/2014/01/salinityandtides2_21.pdf

Schuerch, M., Dolch, T., Bisgwa, J., Vafeidis A.T., 2018. Changing Sediment Dynamics of a Mature Backbarrier Salt Marsh in Response to Sea-Level Rise and Storm Events. Frontiers in Marine Science, 5: 155. https://doi.org/10.3389/fmars.2018.00155

Schuerch, M., Vafeidis, A., Slawig, T., Temmerman, S., 2013. Modeling the influence of changing storm patterns on the ability of a salt marsh to keep pace with sea level rise. Journal of Geophysical Research-Earth Surface, 118 (1), 84-96. https://doi.org/10.1029/2012jf002471

Sinha P.C., Rao Y.R., Dube S.K., 1997. Effect of sea-level rise on tidal circulation in the Hooghly Estuary, Bay of Bengal. Marine Geodesy, 20 (4), 341-366. https://doi.org/10.1080/01490419709388114

Temmerman, S., Bouma, T.J., Govers, G., Wang, Z.B., De Vries, M.B., Herman, P.M.J., 2005. Impact of vegetation on flow routing and sedimentation patterns: Three-dimensional modeling for a tidal marsh. Journal of Geophysical Research-Earth Surface, 110 (F4). https://doi.org/10.1029/2005jf000301

Temmerman, S., Meire, P., Bouma, T.J., Herman, P.M.J., Ysebaert, T., De Vriend, H.J., 2013. Ecosystem-based coastal defence in the face of global change. Nature, 504 (7478), 79-83. https://doi.org/10.1038/nature12859

Tovey, E.L., Pontee, N.I., Harvey, R., 2009. Managed Realignment at Hesketh Out Marsh West. Proceedings of the Institution of Civil Engineers-Engineering Sustainability, 162 (4), 223-228. https://doi.org/10.1680/ensu.2009.162.4.223

Townend, I., Fletcher, C., Knappen, M., Rossington, K., 2011. A review of salt marsh dynamics. Water and Environment Journal, 25 (4), 477-488. https://doi.org/10.1111/j.1747-6593.2010.00243.x

Turner, R.E., Baustian, J.J., Swenson, E.M., Spicer, J.S., 2006. Wetland sedimentation from Hurricanes Katrina and Rita. Science, 314 (5798), 449-452. https://doi.org/10.1126/science.1129116

UKHO, 2001. Admiralty Tide Tables. United Kingdom and Ireland (including European Channel Ports). Taunton: UK Hydrographic Office.

van der Wal, D., Pye, K., Neal, A., 2002. Long-term morphological change in the Ribble Estuary, northwest England. Marine Geology, 189 (3-4), 249-266. https://doi.org/10.1016/s0025-3227(02)00476-0

Van Dongeren, A.R., De Vriend, H.J., 1994. A MODEL OF MORPHOLOGICAL BEHAVIOR OF TIDAL BASINS. Coastal Engineering, 22 (3-4), 287-310.

van Maneen, B., Coco., G., Bryan, K.R., Friedrichs, C.T., 2013. Modeling the morphodynamic response of tidal embayments to sea-level rise. Ocean Dynamics, 63, 1249-1262. https://doi.org/10.1007/s10236-013-0649-6

Van Rijn, L.C., 1993. Principles of sediment transport in rivers, estuaries and coastal areas. Aqua publications, Amsterdam.

von Storch, H., Jiang, W., Furmanczyk, K.K., 2015. Chapter 7 - Storm Surge Case Studies, in: Shroder J.F., Ellis J.T., Sherman D.J. (Eds.), Coastal and Marine Hazards, Risks, and Disasters, Hazards and Disasters Series, pp. 181-196.

Wakefield, R., Tyler, A.N., McDonald, P., Atkin, P.A., Gleizon, P., Gilvear, D., 2011. Estimating sediment and caesium-137 fluxes in the Ribble Estuary through time-series airborne remote sensing. Journal of Environmental Radioactivity, 102 (3), 252-261. https://doi.org/10.1016/j.jenvrad.2010.11.016

Walters, D.C., Kirwan, M.L., 2016. Optimal hurricane overwash thickness for maximizing marsh resilience to sea level rise. Ecology and Evolution, 6 (9), 2948-2956. https://doi.org/10.1002/ece3.2024

Wang, J., Dai, Z., Mei, X., Fagherazzi S, 2020. Tropical Cyclones Significantly Alleviate Mega-Deltaic Erosion Induced by High Riverine Flow. Geophysical Research Letter, 47 (19), e2020GL089065. https://doi.org/10.1029/2020GL089065

Wang, Z.B., Jeuken, M., Gerritsen, H., de Vriend, H.J., Kornman, B.A., 2002. Morphology and asymmetry of the vertical tide in the Westerschelde estuary. Continental Shelf Research, 22 (17), 2599-2609. https://doi.org/10.1016/s0278-4343(02)00134-6

Wolf, J., 1981. Surge-tide interaction in the North Sea and River Thames. In Peregrine, D.H. (Ed.), Floods Due to High Winds and Tides. Elsevier, New York, pp. 75-94.

Zedler, J.B., Kercher, S., 2005. Wetland resources: Status, trends, ecosystem services, and restorability. Annual Review of Environment and Resources, 30, 39-74. https://doi.org/10.1146/annurev.energy.30.050504.144248

Zenghao, Q., Yihong, D., 1996. Numerical Study of Nonlinear Tide-Surge Interaction in the Coastal Waters of Shanghai. Land-Based and Marine Hazards, Advances in Natural and Technological Hazards Research, 7, 139-156. https://doi.org/10.1007/978-94-009-0273-2_9

Zhang, X.H., Leonardi, N., Donatelli, C., Fagherazzi, S., 2020. Divergence of Sediment Fluxes Triggered by Sea-Level Rise Will Reshape Coastal Bays. Geophysical Research Letters, 47 (13). https://doi.org/10.1029/2020gl087862

Declaration of interests

☒ The authors declare that they have no known competing financial interests or personal relationships that could have appeared to influence the work reported in this paper.

☐The authors declare the following financial interests/personal relationships which may be considered as potential competing interests:

Highlights

- Storm surges can positively contribute to the resilience of salt marshes.
- Sea-level rise can threaten the stability of salt marshes.
- Intense storms can counteract the negative impact of sea-level rise.